

ATMOSPHERIC CONVECTION AS A CONTINUOUS PHASE TRANSITION: FURTHER EVIDENCE

OLE PETERS^{*,†} and J. DAVID NEELIN^{†,‡}

**Department of Mathematics, Imperial College London,
180 Queen's Gate and Grantham Institute for Climate Change
London SW7 2AZ UK*

*†Department for Atmospheric and Oceanic Sciences,
University of California Los Angeles, 405 Hilgard Avenue
LA, CA90095-1565, USA*

**ole@santafe.edu*

‡neelin@atmos.ucla.edu

Received 21 October 2009

We present further methods to investigate in how far atmospheric precipitation can be described as a continuous phase transition. Previous work has shown a scale-free range in the rainfall event size distribution and a suggestive power-law pickup in the rain rate above a critical level of instability. Here we examine an additional technique for estimating critical parameters, we investigate the rain rate pickup for an example of an extreme event, namely satellite observations of Hurricane Katrina, and develop an analysis of fluctuations in the rain rate to estimate uncertainties in the tuning parameters relevant for the transition.

Keywords: Critical phenomena; convection; phase transitions.

1. Introduction

Convective rainfall results from the removal of vertical instability in the troposphere, as rising air becomes buoyant relative to its environment, yielding small-scale ($\ll 100$ km) overturning motions, organized in convective plumes. In the simplest scenario, short-wavelength solar radiation heats the surface, resulting in heating and moistening of the atmospheric surface boundary layer, while long-wavelength outgoing radiation cools the upper troposphere. This combination acts to create buoyancy available to convective plumes. This simplest scenario is augmented by interaction with large-scale (e.g., larger than a 100 km model grid cell) atmospheric transports that produce large moisture and energy fluxes which can likewise act to destabilize the column.

The rate at which these large-scale processes create buoyancy is typically slow compared to the rate at which buoyancy can be dissipated by fast-growing convective plumes. Additional fast processes affecting production of rainfall include turbulent entrainment of environmental air into the rising plume, cloud micro-physical

processes including aggregation of droplets and ice crystals, and downdrafts generated by evaporative cooling. Overviews of moist atmospheric convection include Refs. 1, 2, 3. Because of the separation of time scales between the driving and relaxation processes, it has been postulated that the atmosphere is strongly attracted to the point in phase space where convection sets in Ref. 4. This conjecture forms the basis of a class of convective representations in climate models and associated moist atmospheric theory.⁵

At a generic level, it has been argued that slowly driven dissipative systems may display scale-free events of energy release citeJensen1998 and that the attractive state resembles the critical point of a continuous phase transition,⁷ motivating the name “self-organized criticality” (SOC) for scale-free event-size distributions. A number of studies have conjectured that precipitation processes include an element of SOC, based on data analysis in the time domain, noting non-Gaussian fluctuations in various observables⁸; and scale-free distributions of rain event sizes⁹ including power-law regimes over several orders of magnitude.¹⁰

The onset of deep moist convection in observations exhibits properties of a non-equilibrium continuous phase transition,¹¹ with precipitation as the order parameter and column-integrated water vapor as a self-adjusting tuning parameter. Self-organization to the critical region is seen in histograms of the tuning parameter, which peak near criticality. These properties have implications for convective representations in climate models.¹²

Here we summarize the basic hypothesis and present further empirical results. We begin by reviewing in this context generic effects of a separation of scales, scaling, and the relation to phase transitions.

1.1. *Scale freedom from a separation of scales*

A generic source of scale-freedom, and a common feature of SOC systems is a separation of two time scales. Often there are slow driving processes with characteristic scales t_s (for “slow”), and much faster relaxation processes with characteristic time scales $t_f \ll t_s$ (where t_f stands for “fast”). For example, in Manna’s cellular automaton model,¹³ the dynamics imply that for any reasonably defined measure of time, $\lim_{L \rightarrow \infty} (t_f/t_s) = 0$, where L is the system size. In the atmosphere, driving occurs over time scales of days, while rainfall and convection take place on time scales of minutes to hours.

Consider a system with processes operating at N different time scales $t_i | t_{i+1} < t_i$ and an observable $f(t)$, evaluated at some observation time scale t ,

$$f(t) = f(t, t_1, \dots, t_N). \quad (1)$$

If there is a set of fast time scales, bounded from above by t_f and a set of slow time scales, bounded from below by t_s , then, in the limit of $t_f/t_s \rightarrow 0$, there exists a range of time scales t where,

$$\begin{aligned} \forall t_i \leq t_f, \quad t/t_i \rightarrow \infty \quad \text{and} \\ \forall t_i \geq t_s, \quad t/t_i \rightarrow 0. \end{aligned} \quad (2)$$

Comparing f evaluated at observation time scales t' and t for both of which (Eq. 2) holds, yields (following arguments similar to Ref. 14 p. 29 and Ref. 15 p. 17)

$$\frac{f(t')}{f(t)} = \Phi(t'/t, t'/t_1, \dots, t'/t_s, t'/t_f \cdots t'/t_N, t/t_1, \dots, t/t_s, t/t_f \cdots t/t_N) \quad (3)$$

$$\begin{aligned} &\approx \Phi(t'/t, 0, \dots, 0, \infty, \dots, \infty, 0, \dots, 0, \infty, \dots, \infty) \\ &= \Phi(t'/t) \end{aligned} \quad (4)$$

assuming that the function f is well behaved for $t/t_1, \dots, t/t_s, t'/t_1, \dots, t'/t_s \rightarrow 0$ and $t/t_f \cdots t/t_N, t'/t_f \cdots t'/t_N \rightarrow \infty$, and leaving out any constant arguments (the set of arguments $t/t_1, \dots$ is for illustration only – they are implied by the others). The LHS of (Eq. 3) is thus a function, here denoted Φ , that only depends on the ratio of the two observation time scales, t' and t . The assumption of f being well behaved in the relevant limits is strong; without it the generic argument presented here does not apply, meaning that crucial properties are wrapped up into this assumption. Physically, however, the assumption has a clear intuitive interpretation: it corresponds to all processes being either so fast that the system does not respond to the induced fluctuations, or so slow that the induced variations are negligibly small on the observation time scale. The only “orientation”, or sensible unit, left to the observation at time scale t' is the other observation time scale, t . If the arguments leading to (Eq. 4) hold, then $f(t)$ must be a power law. Expressing t' as $t' = at$, (Eq. 3) becomes

$$\frac{f(at)}{f(t)} = \Phi(a), \quad (5)$$

which yields, when differentiated with respect to a ,

$$\frac{tf'(at)}{f(t)} = \Phi'(a), \quad (6)$$

where a prime ($'$) denotes the derivative. The only restriction on a is for it to be close enough to 1 so that (Eq. 2) can hold for both t and t' . It must hold for $a = 1$, in which case (Eq. 6) can be solved for f . Dividing (Eq. 6) by t , recognizing the left-hand side as $d[\ln f(t)]/dt$, integrating and exponentiating yields

$$f(t) \propto t^{\Phi'(1)}, \quad (7)$$

where the constant $\Phi'(1)$ reveals its role as the exponent of the power law.

To summarize, if an observable is affected by processes acting on different scales (e.g., scales of time or space), and two of those scales are separated by an arbitrarily large factor, then there can be a regime where only relative scales are relevant. This is the intermediate asymptotic¹⁵ scaling regime over which a power law of *a priori* undetermined exponent holds.

1.2. *Separation of scales in phase transitions*

Near critical points of continuous phase transitions one can usually identify diverging temporal and spatial correlation lengths, which lead to power-law behavior of spatial and temporal properties. The power laws hold for scales that are small compared to the correlation scale (which may be limited by a finite system size) and large compared to microscopic scales, such as the time scales of the dynamics of individual degrees of freedom or spatial interatomic scales. In this case only relative scales matter and (Eq. 3) applies.

Self-organized critical systems approach the critical point of underlying phase transitions — in the prototypical sandpile models these are absorbing-state (AS) phase transitions.¹⁶ In sandpile models and their AS versions (see Ref. 16) it is possible to investigate both the self-organized critical properties, often avalanches,^{13,17} and the tuned critical properties, often order parameters and their fluctuations.¹⁸ In the following we will investigate both avalanches and order parameter properties for the apparent SOC phase transition associated with atmospheric precipitation.

2. *Scaling in Rainfall*

Section 1 summarizes reasons to expect a scale separation between large-scale atmospheric forcing and scales of convection and rainfall. The scale-free range we focus on now is a range in rain event size. A rain event is here defined as a sequence of non-zero measurements of the rain rate at some point in space, see inset of Fig. 1. The event size is the time-integral of the rain rate over the event, i.e., the water column released during an event. We show here event size distributions from Westermarkelsdorf, on the German Baltic Sea coast, and Nauru Island in the tropical West Pacific. Details of the Baltic coast measurements can be found in Ref. 19 (shown here: measurements in 250 m above ground, averaging time 1 min); the Nauru data set is described in Ref. 20. Rainfall in the tropical West Pacific predominantly comes from deep convective systems, with a typical horizontal extent of individual updraft plumes of a few kilometers. Over the Baltic Sea, on the other hand, much of the rain is generated by propagating cold weather systems that lift warmer airmasses along a front often several hundred kilometers long. Because of these considerably different generating mechanisms it is common to distinguish between convective rainfall and frontal rainfall. The event size distributions in Fig. 1, however, are similar for sizes on the order of 1 mm and smaller despite the different meteorological conditions, with a power-law range over 3–4 orders of magnitude. Tropical rain is often more intense than mid-latitude rain, which may be why the Nauru distribution drops off less quickly for large events. For this tropical case we have investigated the potential underlying phase transition, identifying possible tuning and order parameters and characterizing their behavior.

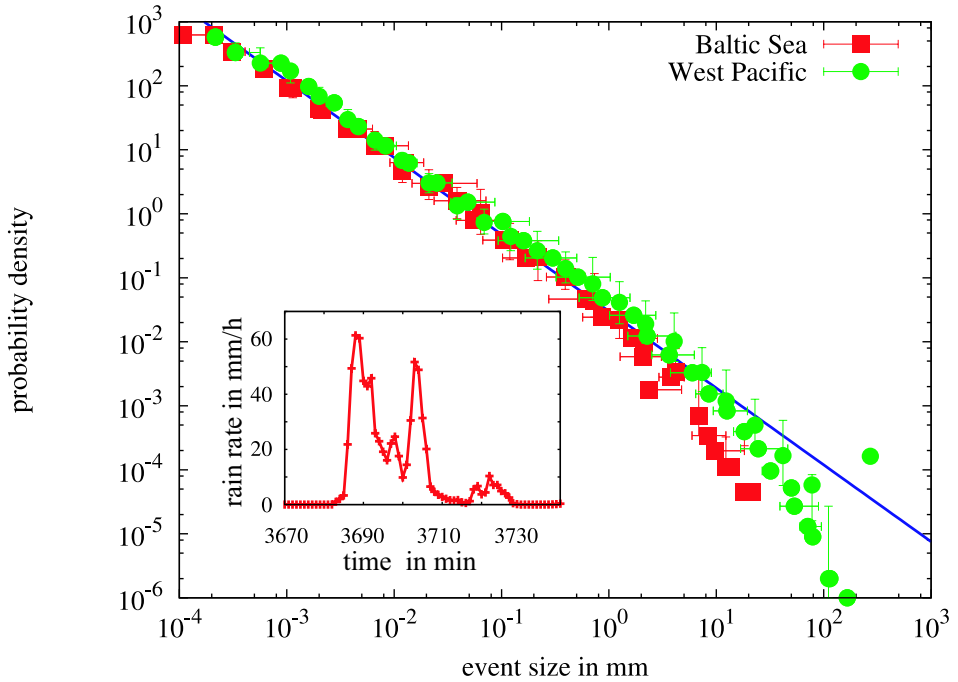


Fig. 1. Event size distributions in Westermarskeldorf (Baltic Sea) and Nauru (Equatorial Pacific). A probability density is estimated for each event (“one-event bins”). Symbols indicate the median, both for fixed event-size bins and for fixed density-bins. Lines indicate 25 and 75 percentiles. The inset illustrates an event, with the event size the area under the red curve.

2.1. Order parameter statistics

Column-integrated water vapor, for which large data sets are available from satellite retrievals, has a strong relationship to the buoyancy available to entraining deep convective plumes²¹ (for given conditions of tropospheric temperature). The column-integrated water vapor is thus a good candidate tuning parameter that controls a phase transition between quiescence and convection with rainfall. We use Tropical Rainfall Measurement Mission (TRMM) Microwave Imager (TMI) data²² with snap-shot estimates of rain rate P and column-integrated water vapor w . The data come in pixels, each about 25 km wide, along swaths traced by the satellite of about 250 km width. Each position on the globe is visited roughly twice per day. Averages of the rain rate, $\langle P \rangle(w)$ conditioned on the prevalent water vapor being within 0.3 mm bins were computed. Above a critical value w_c , they are well described by

$$\langle P \rangle(w) = a^j (w - w_c^j)^\beta, \quad \text{for } w > w_c. \quad (8)$$

The amplitudes a^j and critical values w_c^j are non-universal. In Ref. 11, where temperature information was not available, these were determined for different climatic regions (for instance East Pacific versus West Pacific). As expected, the exponent

β shows little fluctuation and no discernible dependence on climatic region. The issues in determining β will be discussed below. We note here that our estimates of β from different ocean basins and different temperature ranges are consistent with the hypothesis of it being a universal exponent. Other properties of the continuous phase transition, such as finite-size scaling of the precipitation variance are given in Ref. 11.

Temperature is fundamentally as important as water vapor to the transition, but temperature variations within a given region in the tropics are small compared to water vapor variations. In recent studies,^{12,23} leading effects of temperature are included via a mass-weighted vertical average temperature, \hat{T} , from the reanalysis data set ERA-40.²⁴

These studies suggest that the transition occurs at a temperature-dependent critical point $w_c(\hat{T})$ which is independent of the tropical region, and quantitatively important for climate models. Using data from Ref. 23 (averages of the rain rate, conditioned both on w being within a 0.3 mm bin and the \hat{T} being within a 1 K bin), we further examine this transition.

With \hat{T} constant, (Eq. 8) holds, as illustrated in Fig. 2. Fitting the power law (Eq. 8) to the data shown in Fig. 2 above w_c requires the adjustment of three parameters: a , w_c , and β , which are related non-linearly. Since the fit is expected to hold in an *a priori* unspecified interval $[w_{\min}, w_{\max}]$, some criterion for selecting w_{\min} and w_{\max} must also be specified. In principle, visual inspection should provide a good intuition for the validity of (Eq. 8). But linear scales are problematic because linearly small deviations from the relation might be logarithmically large; using double-logarithmic scales (i.e., showing $\ln(\langle P \rangle(w))$ vs. $\ln(w - w_c)$) comes at the cost of fixing w_c . If the estimate of w_c is incorrect, conclusions about β and a will be affected. A method, sometimes called “d-log Padé method”, that visually represents the uncertainties involved and is less laden with assumptions and parameter estimates was used by Baker²⁵ and further described e.g., by Kouvel and Fisher²⁶: Dividing (Eq. 8) by minus its derivative, one obtains

$$\frac{\langle r \rangle(w)}{-d\langle r \rangle(w)/dw} = \frac{w_c - w}{\beta}. \quad (9)$$

The amplitude a from (Eq. 8) cancels, and the quantity in (Eq. 9) is linear in w . The procedure is equivalent to considering logarithmic slopes, as the left-hand side of (Eq. 9) is the inverse of the derivative of $\ln \langle P \rangle(w)$. A weakness of this method is that the required derivative amplifies noise, notably at high w values, where in our case the available ensemble becomes small; here the derivative is estimated using a five-point central difference to reduce this. Figure 2 displays this quantity (crosses \times), observed at $\hat{T} = 271K$ in the West Pacific. The critical point of the transition, $w_c(\hat{T})$, is immediately relevant to climate modeling as discussed in Ref. 12. Estimating (Eq. 9) provides an appropriate visual representation of the uncertainties involved.

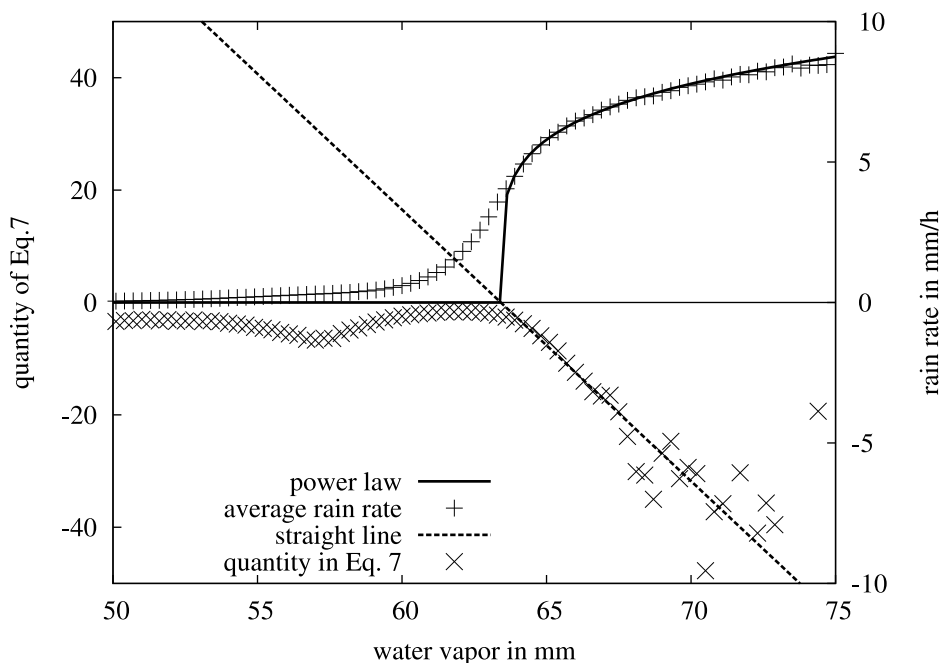


Fig. 2. Order parameter pick-up for a region in the West Pacific at $\hat{T} = 271$. Plus signs (+) mark conditionally averaged rain rates, expected to approximate (Eq. 8) (here represented by a solid line) for $w > w_c$. Crosses (\times) show measurements of the left-hand side of (Eq. 9), with a dashed straight line following the right-hand side of (Eq. 9) fitted to it. The solid and dashed lines correspond to the same w_c and β . The quality of the fit is best judged visually in the linear rendering (dashed line and crosses \times). Best-fit parameters depend on the choice of the fitting range, here $63.5 \text{ mm} \leq w \leq 68 \text{ mm}$. We find $\beta \approx 0.21$ and $w_c \approx 63.4$ from a χ^2 -fit of the data vs. the right-hand side of (Eq. 9).

2.2. Rainfall in a hurricane

Out of curiosity and to determine the universality of the observed dependence $\langle P \rangle(w)$, we picked a sample of data points where most of the strong precipitation occurred inside a Hurricane, here Hurricane Katrina, 2005. We did not stratify by temperature since the statistics are much poorer in this small data set. Due to the relatively frequent occurrence of strong rainfall and high water vapor in the sample, it is nonetheless possible to observe a dependence similar to (Eq. 8) with some statistical significance, see Fig. 3. The hurricane, by this measure, does not look fundamentally different from deep convective rain from less organized weather systems.

3. Order Parameter Fluctuations

Extending the analogy with continuous phase transitions, we study the fluctuations of the order parameter, $\sigma_P = (\langle P^2 \rangle - \langle P \rangle^2)^{1/2}$. As reported in Ref. 11, σ_P is found

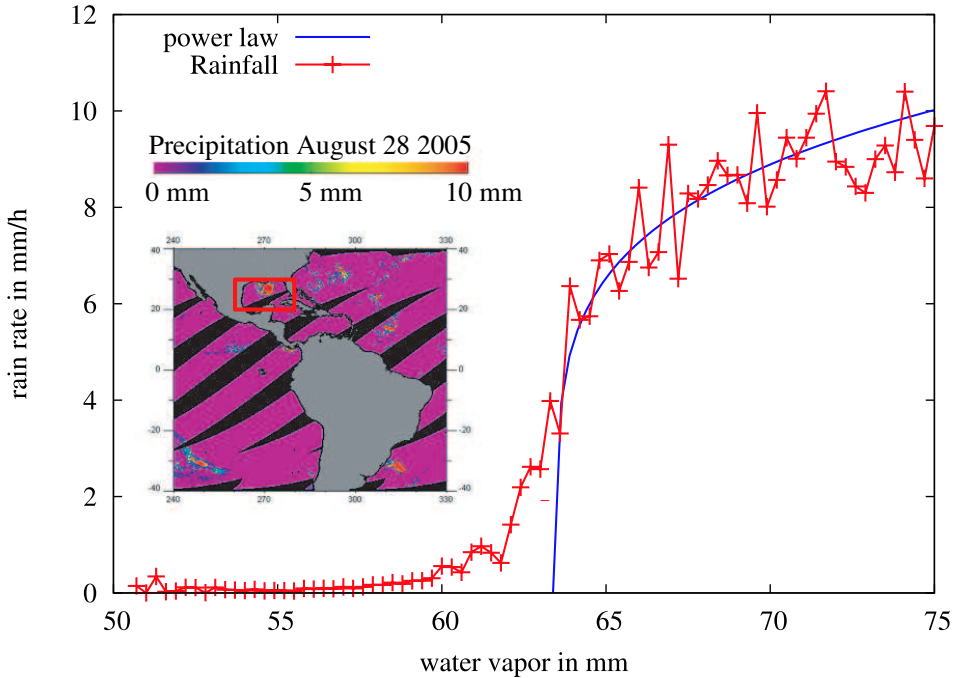


Fig. 3. Conditionally averaged rain rate in a sample of satellite pixels containing measurements of Hurricane Katrina, including all temperatures: Gulf of Mexico (red box, 80W to 100W, 20N to 30N), August 28 till September 02 2005. Red crosses are data, and the blue line corresponds to (Eq. 8) using $\beta = 0.21$, as estimated in Fig. 2.

to peak strongly near the critical point w_c . This peak becomes sharper when we control for \hat{T} .¹² Quantifying the error in the tuning parameter (and optimizing its estimation) has considerable practical benefits in atmospheric applications²³; the following considerations are relevant to this task.

We first treat the well-known case of an equilibrium phase transition in the canonical ensemble. In a spin system with order parameter m (magnetization), we expect $L^{d/2}\sigma_m$ to diverge as the tuning parameter (temperature) approaches its critical value, $T \rightarrow T_c$, such that

$$\sigma_m^{\text{critical}} \propto |T_c - T|^{-\gamma/2}, \tag{10}$$

where \propto refers to the leading-order behavior up to a system-size dependent maximum. In a real system whose order parameter behaves according to (Eq. 8), a small measurement error, or small fluctuations, in the tuning parameter, ΔT , would lead to a similar divergence (within measurement limits), such that

$$\sigma_m^{\text{tuningerror}} = \partial_T \langle m \rangle \Delta T \propto |T_c - T|^{\beta-1} \Delta T, \tag{11}$$

as evident from the low-temperature behavior, $T < T_c$. Here we ask how the two types of (capped) divergence, (Eq. 10) and (Eq. 11), are related.

Equation (10) and (Eq. 11) describe different scaling behaviors if $-\gamma/2 \neq \beta - 1$; according to Rushbrook’s scaling law,²⁷

$$-\gamma/2 = \beta - 1 + \alpha/2, \tag{12}$$

meaning that the scaling behaviors are identical if $\alpha = 0$. For a given system size, the quantity

$$\frac{(\langle m^2 \rangle - \langle m \rangle^2)^{1/2}}{\partial_T \langle m \rangle} \propto (T_c - T)^{-\gamma/2 - \beta + 1} (= \alpha/2, \text{ by Rushbrooke}), \tag{13}$$

which measures the magnitude of fluctuations in m relative to the steepness of $\langle m \rangle (T)$, will peak, be flat, or have a minimum at T_c , depending on the value of α . There are well-known examples for all three possibilities, $\alpha < 0, = 0, > 0$: in the 3-dimensional Heisenberg model, $\alpha_H \approx -0.12$, in the 2- d Ising model, $\alpha_I = 0$, and in the 2- d 3-states Potts model $\alpha_P = 1/3$.

The exponent α controls the scaling behavior of the energy fluctuations, so how is the steepness of the expectation value of the order parameter in T related to energy fluctuations? We compute the denominator of (Eq. 13),

$$\begin{aligned} \partial_T \langle m \rangle &= \partial_T \frac{\sum_i m_i \exp(-E_i/(k_B T))}{Z} \\ &= \frac{1}{k_B T^2} (\langle mE \rangle - \langle m \rangle \langle E \rangle). \end{aligned} \tag{14}$$

where sums are over all states i , and magnetizations and energies E are labelled accordingly. k_B is Boltzmann’s constant, $Z = \sum_i \exp(-E_i/(k_B T))$ is the canonical partition sum.

Thus, in the canonical ensemble, the expectation value of some quantity, differentiated with respect to the temperature, is proportional to the covariance of that quantity with the energy. A fluctuating energy (due to contact with a heat bath) and a fluctuating temperature are virtually indistinguishable. The temperature only enters into the partition sum through $E/(k_B T)$, i.e., as an energy scale. The equivalence of tuning-parameter fluctuations and energy fluctuations remains intact in the critical limit if the energy fluctuations neither diverge (at most logarithmically) nor vanish (i.e., $\alpha = 0$).

Measuring the standard deviation of an order parameter in a real system can thus reveal imperfections in the control of the tuning parameter. Returning to the case of rainfall, it is unclear to what the energy and hence (Eq. 14) correspond, but the tuning-parameter derivative of the order parameter can be estimated from the data. A measured value $\sigma_P^{\text{measured}}(w)$ (at fixed \hat{T}) will essentially be a sum of two contributions,

$$\sigma_P^{\text{measured}}(w) = (\langle P^2 \rangle (w) - \langle P \rangle (w)^2)^{1/2} + \partial_w \langle P \rangle (w) \Delta w, \tag{15}$$

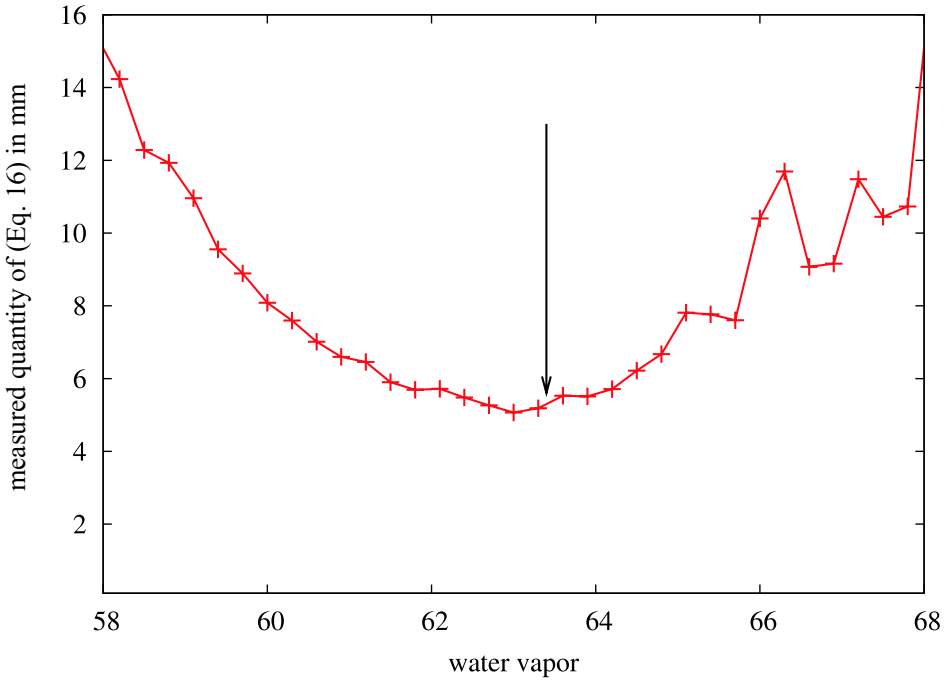


Fig. 4. The measured standard deviation, $\sigma_r^{\text{measured}}$ of the rain rate, divided by the slope $\partial_w \langle P \rangle (w)$. The arrow indicates the position of the critical point, which is close to the minimum, suggesting $\alpha > 0$, and $\Delta w \approx 5$ mm.

where Δw is the imperfection in the control of the relevant tuning parameters, expressed as a water vapor. Assuming that errors in the measured slope are negligible, i.e., $\partial_w \langle P \rangle (w) = \partial_w^{\text{measured}} \langle P \rangle (w)$, we divide by our estimate of $\partial_w \langle P \rangle (w)$ to obtain

$$\frac{\sigma_P^{\text{measured}}(w)}{\partial_w \langle P \rangle} = \frac{(\langle P^2 \rangle (w) - \langle P \rangle (w)^2)^{1/2}}{\partial_w \langle P \rangle} + \Delta w \tag{16}$$

The first term on the right-hand side of (Eq. 16) corresponds to (Eq. 13) and either peaks ($\alpha < 0$), is constant ($\alpha = 0$) or dips ($\alpha > 0$) as the tuning parameter approaches the critical value from the ordered phase, here $w > w_c$. If it dips strongly, we are left with only the second term, an estimate for the imperfection in the tuning parameter. In Figure 4, this quantity decreases as one moves toward the critical point, suggesting that in the case of rainfall, “ $\alpha > 0$ ”, in the sense that the first term on the RHS of (Eq. 16) dips strongly. The quantity of (Eq. 16) has a minimum near the critical point, with a value of about $\Delta w \approx 5$ mm. This is in agreement with previous estimates of the uncertainty in the measured tuning parameter, here expressed as water vapor.²³

4. Conclusion

Further tests are presented of an analogy between rainfall and convection in the atmosphere and continuous phase transitions. We summarize arguments on general grounds that a large separation of scales can lead to a scale-free intermediate asymptotic regime. Scale-free rain event size distributions are indeed found in the atmosphere where a slow driving time scale is separated from a much faster time scale of energy dissipation. Here, we note the similarity, over four orders of magnitude, between two such distributions, one from a tropical site and one from a mid-latitude site, with rather different large-scale climate regimes. Differences between the distributions are found primarily at large event sizes, where the tropical distribution drops off less quickly. The similarity appears consistent with the separation between large-scale forcing and the short timescale processes (convection, turbulence and cloud micro-physics) leading to precipitation, although a single meteorological process associated with the power-law exponent is not identified.

We further examine the sudden pickup above a critical value of column water vapor in satellite microwave retrievals. A manipulation that renders the power law portion of this pickup linear and independent of the amplitude parameter allows a realistic visual rendering of uncertainties. Estimates of the power law parameters w_c and β are consistent with our prior results. Examination of the pickup for an example of an extreme meteorological event (hurricane Katrina) suggests that the basic properties are similar even in this regime. Finally, we compare critical order parameter fluctuations to fluctuations in the expectation value of a near-critical order parameter due to uncertainties in the tuning parameter. This makes it possible to estimate the uncertainties in the tuning parameter, expressed as a column water vapor in the TMI data set, combined with ERA-40 data, as about 5 mm or 1% of the critical value.

Acknowledgments

This work was supported under National Science Foundation ATM-0082529 and National Oceanic and Atmospheric Administration NA05-OAR4310007 and NA08OAR4310882. JDN acknowledges sabbatical support from the J. S. Guggenheim Foundation. OP would like to thank B. Stevens for hospitality at MPI-Hamburg, where part of this manuscript was prepared. TMI data are produced by Remote Sensing Systems and sponsored by the NASA Earth Science Reason Discover Project. We thank K. Hales for assistance with data sets from a related project still in the publication process, C. Holloway for discussions and assistance with the Nauru data, and G. Pruessner for discussions regarding Sec. 3.

References

1. R. A. J. Houze, *Cloud Dynamics*. Academic Press Inc, San Diego, 1993.
2. K. A. Emanuel, *Atmospheric Convection*. Oxford University Press, 1994.

3. B. Stevens, "Atmospheric moist convection," *Annu. Rev. Earth Planet. Sci.*, vol. 33, pp. 605–643, 2005.
4. A. Arakawa and W. H. Schubert, "Interaction of a cumulus cloud ensemble with the large-scale environment, part i," *J. Atmos. Sci.*, vol. 31, pp. 674–701, 1974.
5. K. A. Emanuel, J. D. Neelin, and C. S. Bretherton, "On large-scale circulations in convecting atmospheres," *Quart. J. Roy. Met. Soc.*, vol. 120, no. 519, pp. 1111–1143, 1994.
6. H. J. Jensen, *Self-Organized Criticality: Emergent Complex Behavior in Physical and Biological Systems*. Cambridge University Press, 1998.
7. C. Tang and P. Bak, "Critical exponents and scaling relations for self-organized critical phenomena," *Phys. Rev. Lett.*, vol. 60, pp. 2347–2350, June 1988.
8. G. Vattay and A. Harnos, "Scaling behavior in daily air humidity fluctuations," *Phys. Rev. Lett.*, vol. 73, pp. 768 – 771, August 1994.
9. R. F. S. Andrade, H. J. Schellnhuber, and M. Claussen, "Analysis of rainfall records: possible relation to self-organized criticality," *Physica A*, vol. 254, pp. 557–568, 1998.
10. O. Peters, C. Hertlein, and K. Christensen, "A complexity view of rainfall," *Phys. Rev. Lett.*, vol. 88, p. 018701, January 2002.
11. O. Peters and J. D. Neelin, "Critical phenomena in atmospheric precipitation," *Nature Phys.*, vol. 2, pp. 393–396, June 2006.
12. J. D. Neelin, O. Peters, J. W.-B. Lin, K. Hales, and C. E. Holloway, "Rethinking convective quasi-equilibrium: observational constraints for stochastic convective schemes in climate models," *Phil. Trans. R. Soc. A*, vol. 366, pp. 2581–2604, 2008.
13. S. S. Manna, "Two-state model of self-organized criticality," *J. Phys. A*, vol. 24, pp. L363–L369, 1991.
14. M. Le Bellac, *Quantum and Statistical Field Theory*. Oxford University Press, 1991.
15. G. I. Barenblatt, *Scaling*. Cambridge University Press, 2003.
16. R. Dickman, M. A. M. noz, A. Vespignani, and S. Zapperi, "Paths to self-organized criticality," *Braz. J. Phys.*, vol. 30, no. 1, pp. 27–41, 2000.
17. S. Lübeck, "Moment analysis of the probability distribution of different sandpile models," *Phys. Rev. E*, vol. 61, pp. 204–209, January 2000.
18. R. Dickman, M. Alava, M. M. noz, J. Peltola, A. Vespignani, and S. Zapperi, "Critical behaviour of a one-dimensional fixed-energy stochastic sandpile," *Phys. Rev. E*, vol. 64, p. 056104, 2001.
19. G. Peters, B. Fischer, and T. Andersson, "Rain observations with a vertically looking micro rain radar (mrr)," *Boreal Env. Res.*, vol. 7, pp. 353–362, 2002.
20. J. H. Mather, T. P. Ackerman, W. E. Clements, F. J. Barnes, M. D. Ivey, L. D. Hatfield, and R. M. Reynolds, "An atmospheric radiation and cloud station in the tropical western pacific," *Bull. Amer. Meteor. Soc.*, vol. 79, no. 4, pp. 627–642, 1998.
21. C. E. Holloway and J. D. Neelin, "Moisture vertical structure, column water vapor, and tropical deep convection," *in press, J. Atmos. Sci.*, 2009.
22. K. A. Hilburn and F. J. Wentz, "Intercalibrated passive microwave rain products from the Unified Microwave Ocean Retrieval Algorithm (UMORA)," *J. Appl. Meteor. Clim.*, vol. 47, pp. 778–794, 2008.
23. J. D. Neelin, O. Peters, and K. Hales, "The transition to deep convection," *to appear in J. Atmos. Sci.*, 2009.
24. S. M. Uppala and coauthors, "The era-40 re-analysis," *Quart. J. Roy. Met. Soc.*, vol. 131, no. 612, pp. 2961–3012, 2005.
25. G. A. Baker Jr., "Application of the Padé approximant method to the investigation of some magnetic properties of the Ising model," *Phys. Rev.*, vol. 124, pp. 768–774, November 1961.

26. J. S. Kouvel and M. E. Fisher, "Detailed magnetic behavior of nickel near its curie point," *Phys. Rev.*, vol. 136, no. 6A, pp. A1626–A1632, 1964.
27. H. B. Callen, *Thermodynamics and an introduction to thermostatistics*. Wiley, 2 ed., 1985.